

CRITICAL DEFORMATION UNDER SHEAR-TENSION LOADING IN MULTISTAGE PROCESSES

M.P. Sklad^①, E. Atzema^②, F. Schouten^②, M. de Bruine^② and J. Verhaeghe^③

^①Dept. of Mechanical Engineering,
McMaster University
Hamilton, Ontario, L8S 4L7, Canada
e-mail: sklad@mcmaster.ca

^②Corus Research Development & Technology
PO Box 10000, 1970 CA IJmuiden, The Netherlands
e-mail: eisso.atzema@corusgroup.com, frank.schouten@corusgroup.com, menno.de-bruine@corusgroup.com

^③FMTI Systems,
1063 King St. W.
Hamilton, Ontario, L8H 4S3, Canada
e-mail: joev@fmtisystems.com

ABSTRACT

The experimental method for determining forming limits in sheet material undergoing two stage deformation processes is presented. The method utilizes samples exhibiting a variety of deformation paths and strain magnitudes induced at the first stage which are brought to fracture at the second stage. The paper reveals, experimentally, the effect of deformation history on fracture in the material, whether occurring along a plane aligned with the principal directions of deformation or along a plane exhibiting tension-shear loading which is not aligned with the principal directions of deformation. The experimental failure strain data are translated to the stress space and the existence of a tension-shear stress forming limit is considered.

Keywords: Strain and Stress Forming Limit Diagram; Shear-tension failure; Multistage process; Grid strain analysis.

1. INTRODUCTION

The subject of formability of sheet metal specifically in multistage processes is of major importance. Nearly all industrial sheet metal forming applications employ multistage deformation procedures. Such processes may involve a series of operations resulting in a non-proportional deformation of the sheet material. The strain path and/or the orientation of the principal directions of deformation in the material configuration may be different at each stage of the process. The presence of a non-proportional deformation rules out the direct use of the conventional forming limit diagram, FLD, for evaluating forming severity because, in general, the principal strains used in the FLD are not additive. The deficiency of the FLD is eliminated by the concept referred to as the stress forming limit diagram, SFLD, which depicts the material failure condition in terms of the principal stresses instead of the principal strains used in the FLD, [1-3]. The rationale of the SFLD is in the hypothesis of the existence of a specific stress state at which the material fails. This stress state can be determined using the proportional deformation, i.e. FLD, which is translated using the constitutive law into the stress space, SFLD, and may subsequently be applied to detect that critical stress state under non-proportional deformation conditions to which the FLD does not apply. Although direct measurements of the stresses in forming processes are very limited or impossible, the calculated SFLD is readily available for forming severity evaluation in numerical forming process simulation based on the finite element method in which the calculation of the stress state is an integral component of the numerical procedure. In the context of the numerical simulation of non-proportional deformation processes, the forming severity evaluated based on the SFLD can be communicated in the familiar form of a point on the traditional FLD [4]. However in this case the major-minor strain point on the FLD is not interpreted as the actual strain state, but as a hypothetical proportional deformation strain state resulting in the same stress state as the stress state calculated for the non-proportional deformation. On the FLD, the slope of the equivalent strain path is based on the stress state taken from the SFLD while the magnitude of equivalent proportional strains accounts for the effects of deformation history. The concept of equivalent FLD derived from SFLD is illustrated in figure 1.

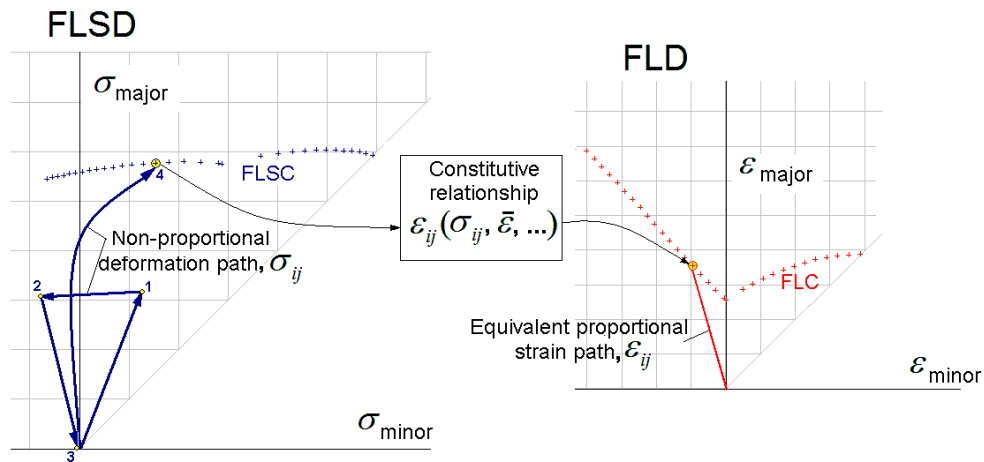


Figure 1. Concept of equivalent FLD for non-proportional deformation derived from SFLD

The effect of the pre-strain magnitude, path and changes of straining directionality on forming limits in multistage processes were examined experimentally for a range of combinations of deformation parameters in [5]. The work cited confirmed the validity of the SFLD and showed that changes in the deformation directionality had no noticeable effect on the formability of the material being tested.

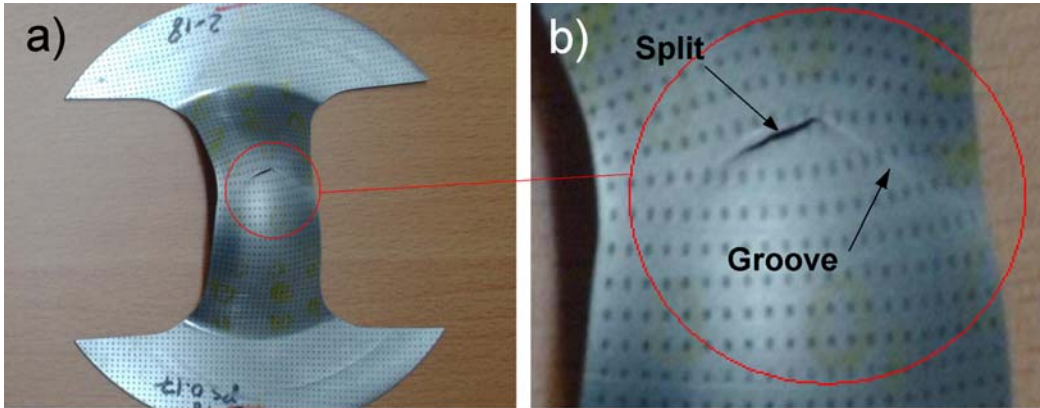


Figure 2. Nakazima dome test sample with geometry of the shaft producing uniaxial tension and the material failure zone

Figure 2 illustrates an example of the failure zone on a Nakazima dome test sample with the geometry of the shaft producing the uniaxial tension path used in the experimental study cited above. The material of this particular sample was initially prestrained with the effective strain reaching a magnitude of 0.17 under the plane strain path. The failure zone shows a groove and the split. Orientation of the groove is about 50° from the tension direction, which is roughly consistent with the “zero extension” direction of 54.7° as predicted by Hill [6]. However the actual split of the material occurred along a different direction which is neither the zero extension nor the principal direction. The deformation along the split line shown in figure 2 must comprise tension combined with shear stress and shear distortion components which cannot be depicted by means of the FLD or the SFLD which are based on principal directions.

This paper examines, experimentally, the failure of material under shear-tension.

2. MATERIALS

2.1 Properties

The material used in this study was Corus steel DX54D+Z (designation according to EN 10327). This is a hot-dip zinc coated steel for forming. The mechanical properties of the specific coil used are listed in table 1. This material shows strong normal anisotropy accompanied by some planar anisotropy indicating good deepdrawability, albeit with some earing. The FLD and the forming limit curves, FLC, are given in figure 3. In figure 3 the continuous line represents an experimentally measured FLC using the Corus RD&T procedure AUT-STN-002 which conforms to the then current but now obsolete ISO 12004:1997 [7]. Corus RD&T has since moved on to ISO 12004-2:2008. For comparison the dotted line represents the FLC calculated according to the Keeler-Brazier, KB, formula [8] for thickness, 0.815mm, and the average n -value of 0.219.

Table 1. – Mechanical properties of the test material

Thickness [mm]	direction [deg]	Rp [MPa]	Rm [MPa]	A80 [%]	r	n
0.815	0	163	297	46.0	2.171	0.226
	45	172	304	43.8	1.849	0.215
	90	169	293	47.4	2.575	0.220

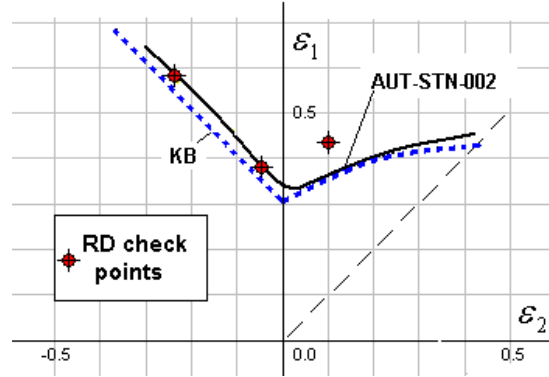


Figure 3. FLC curves plus FLC RD check points

2.2 Sample preparation

The Nakazima dome test samples used to investigate the failure of a material under shear-tension, consisted of a pre-strained material extracted from a production part as described in [5]. The initial production part blank was electro-etched with a 2 mm polka dot grid needed for strain measurements induced after the pre-straining stage and after the failure of the material in the Nakazima dome test. The etched grid was aligned with the rolling direction of the sheet.

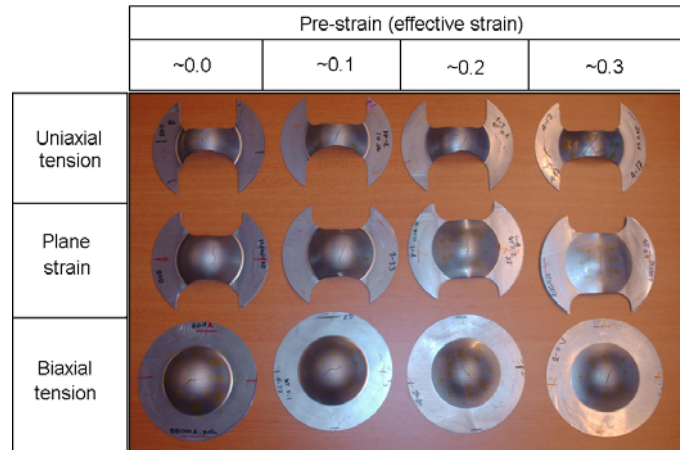


Figure 4. Fractured Nakazima dome test samples

Three geometries of the Nakazima 75mm dome diameter test samples were used, targeting uniaxial tension, plane strain and biaxial tension straining paths. The edges of the shaft section of

the samples were deburred and polished. Figure 4 shows a matrix of deformed samples arranged by geometry type and by the approximate magnitude of prestrain measured in terms of the effective strain.

3. EXPERIMENTAL PROCEDURE

3.1 Nakazima dome tests

The Nakazima dome tests were performed on an Erichsen cupping press, at a low punch speed using manual press control. A disposable polymer disk was used between the blank and the punch, and the punch and the blank were dry. The tests were manually terminated at the first appearance of a groove and/or fracture.

3.2 Deformation measurements and calculations

All deformation measurements were conducted off-line based on the measurement of distortion of the polka dot grid etched on the sheet surface. The surface strains were measured using a FMTI grid analyzer. In order to account for the effect of the deformation history leading to the failure in the Nakazima dome test, the deformation at the same material failure point was measured twice - first on the prestrained material, extracted from the production part and then, on the fractured Nakazima dome sample. Strain measurements performed off-line call for the assumption of proportional deformation applied separately at each deformation stage. The parameters of the deformation determined directly from the image of the distorted grid consisted of the increment of principal strains, orientation of the principal directions of deformation in reference to the rolling direction of the sheet and the orientation of the fracture in reference to the principal directions of the deformation, as shown in figure 5.

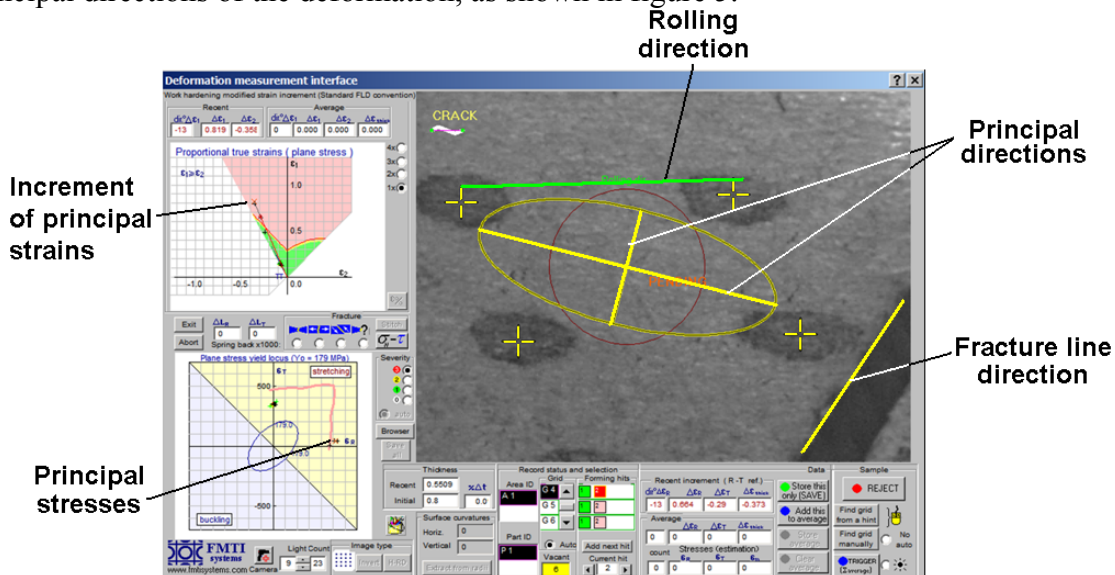


Figure 5. Deformation measurement interface window of the grid analyzer

Other characteristics of the deformation pertaining to the stress state, such as principal stresses and fracture stresses were calculated by applying the constitutive law to the strain increments and performing transformation of the principal stresses to the fracture plane. The

calculation of principal stresses employs the stress-strain curve, $\sigma(\varepsilon)$, interpolated by the exponential equation:

$$\sigma = 521 \varepsilon^{0.219} \text{ [MPa]}, \quad (1)$$

and the flow rule for an anisotropic material with the average plastic strain ratio, $\bar{r} = 2.111$, for the material used. Transformation of principal stresses to the fracture plane direction, ϕ , is performed using Mohr's circle equations in two dimensions:

$$\begin{aligned} \sigma_{xx} &= \frac{1}{2}(\sigma_1 + \sigma_2) + \frac{1}{2} \cos(2\phi)(\sigma_1 - \sigma_2), \\ \sigma_{yy} &= \frac{1}{2}(\sigma_1 + \sigma_2) - \frac{1}{2} \cos(2\phi)(\sigma_1 - \sigma_2), \\ \tau_{xy} &= -\frac{1}{2} \sin(2\phi)(\sigma_1 - \sigma_2). \end{aligned} \quad (2)$$

4. RESULTS

If present, the material fracture along a non-principal direction often appears to be at an angle approaching 22.5° to the minor principal direction of deformation. Two such samples, one with geometry anticipating failure under uni-axial tension and the other one designed for the plane strain path are shown in figure 6. Both samples were prestrained with an effective strain of ~ 0.1 . There are no noticeable grooves in the zero extension directions on either of these samples. Formation of the fracture along the direction inclined at an approximately 22.5° angle to the minor principal direction. The in-plane stresses, σ_{xx}, τ_{xy} , reach a maximum along the 22.5° direction. The fracture along the 22.5° direction was persistent on all uniaxial tensile samples.

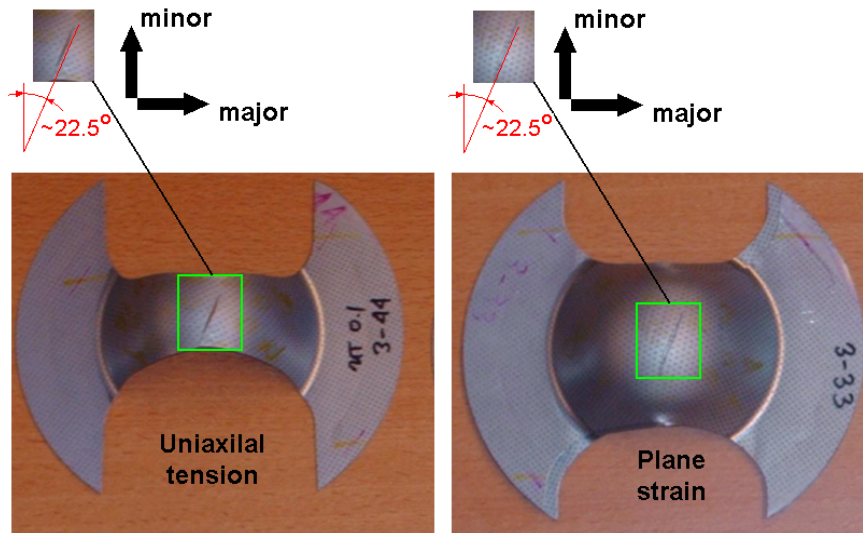


Figure 6. Nakazima dome samples with fracture at a 22.5° angle to the minor principal direction of deformation

However for the plane strain samples this behavior was observed only on samples moderately prestrained, up to 0.1 effective strain. More severely prestrained plane strain samples developed fractures along the zero extension direction which in this case is the minor principal direction. The comparison of the fracture modes observed on the plane strain and uniaxial tension samples subjected to a different level of prestrain is given in figure 7.

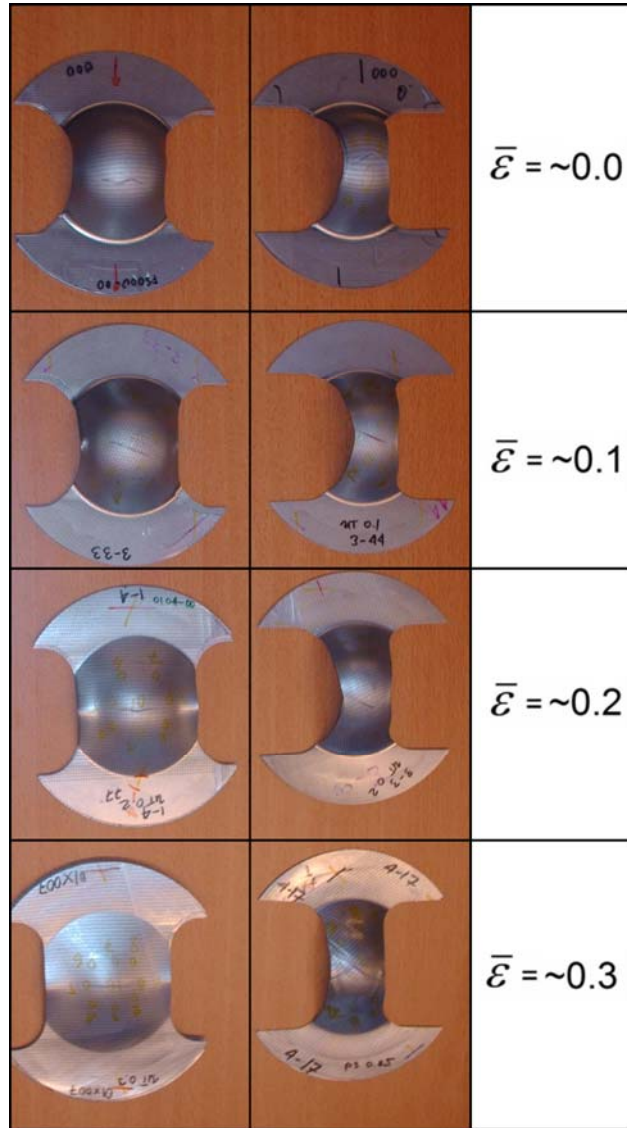


Figure 7. Comparison of fracture modes on plane strain and uniaxial tension samples

A somewhat similar change of the fracture mode has been noticed on the samples subjected to biaxial tension, shown in figure 8. A realistic biaxial stretching process may depart from the ideal true equibiaxial tension and develop distinct principal directions in the sheet plane. In figure 8 the fracture along a zigzag line on samples with small prestrain is consistent with the fracture observed on the plane strain samples while this behavior vanishes with an increase of the prestrain.

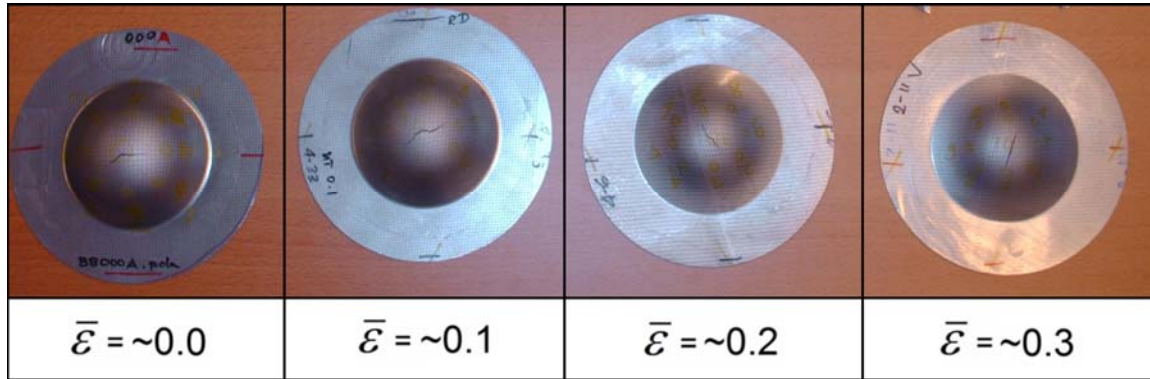


Figure 8. Fracture modes of biaxial tension samples

5. DISCUSSION

The fracture condition is represented by the stress and strain state on a plane along which the material fractures at the instant of failure. The traditional concepts of FLD and SFLD describe the failure condition in terms of principal strains and stresses respectively. However FLD and SFLD do not directly capture the fracture condition occurring along a direction other than the principal direction of deformation. The strain and stress state along non-principal directions always consists of normal and tangential components. Therefore, the prime failure condition for a fracture along a non-principal direction must be expressed in terms of the normal and tangential components of deformation which, in the case of multistage sheet forming processes, are the stress components, σ_{xx}, τ_{xy} present on the fracture plane. The stress components, σ_{xx}, τ_{xy} , cannot be measured directly. They have to be calculated from the measured strain increments as described above in section 3.2.

Table 2. – Fracture stresses

Sample	σ_{major} [MPa]	σ_{minor} [MPa]	Fracture plane angle [°]	σ_{xx} [MPa]	τ_{xy} [MPa]
1	525	66	23	457	163
2	656	315	23	604	122
3	635	280	18	603	102
4	548	250	8	542	43
5	584	195	5	581	32
6	571	245	7	566	38
7	545	215	24	490	123
8	513	43	19	462	146
9	488	454	46	471	17

Table 2 lists fracture stresses determined for nine randomly selected Nakazima test samples. The fracture stresses were calculated using the algorithms and the fracture plane angle measurements available within the grid analyzer. Figure 9 illustrates, graphically, the fracture stresses listed in table 2. In figure 9, the fracture stress states are shown side by side in terms of the principal stresses, $(\sigma_{major}, \sigma_{minor})$, and the normal and shear stresses along the fracture plane,

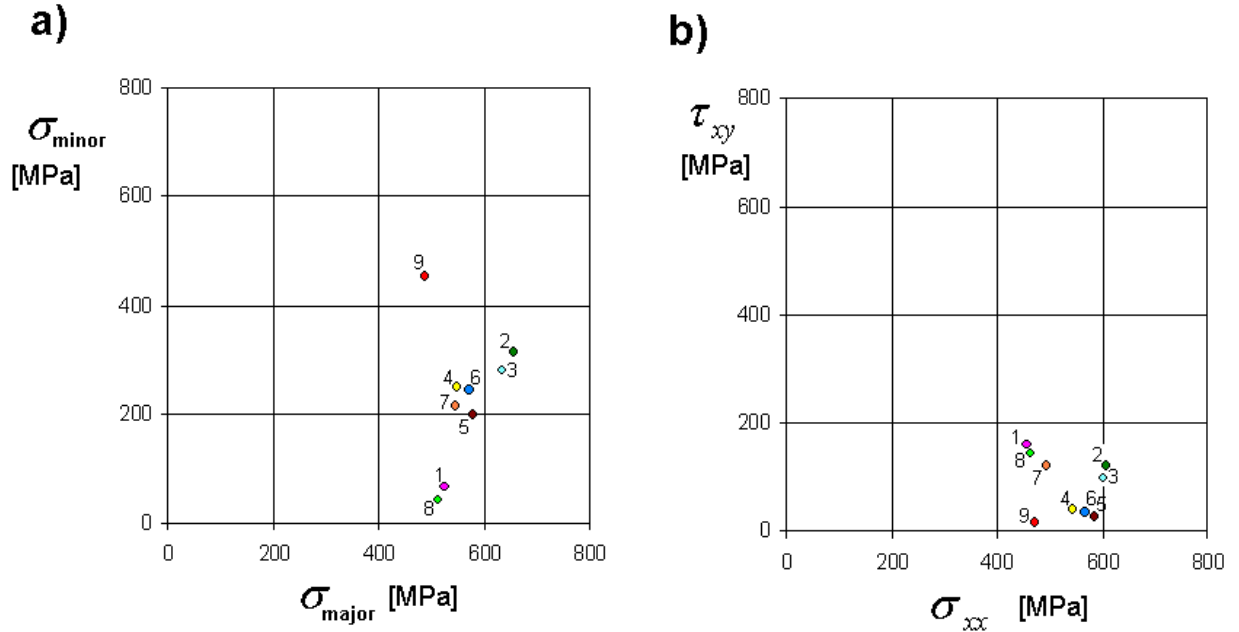


Figure 9. Fracture stresses in: a) – expressed in principal configuration, $\sigma_{\text{major}} - \sigma_{\text{minor}}$
 b) – expressed in fracture plane configuration, $\sigma_{xx} - \tau_{xy}$

(σ_{xx}, τ_{xy}). The normal-shear stress diagram, $\sigma_{xx} - \tau_{xy}$, shown in figure 9b, is employed by the classical Coulomb-Mohr failure theory for brittle materials [9]. However here each of the points representing the fracture stresses, σ_{xx} and τ_{xy} , is calculated using the direction of the fracture plane in the material configuration measured experimentally. With the implied inclusion of the fracture plane direction, the fracture stresses, σ_{xx} and τ_{xy} , appear to be grouped together in one region of the, $\sigma_{xx} - \tau_{xy}$, diagram. This observation could suggest a hypothesis that a stress fracture criterion based on a simple tension-shear stress state rather than principal stress components may exist for sheet metal subjected to multistage deformation processes.

The experimental procedure presented in this paper where a material prestrained in a production forming process, is subjected to the Nakazima dome test, was primarily aimed at obtaining SFLD for a large variety of deformation sequences as reported in [5]. The shortcoming of this procedure is that a non-uniform deformation induced at the first stage during forming of the production part is carried on to the second stage and may initiate significant deformation gradients in the proximity of the fracture as shown in figure 2b. The length of two adjacent grid elements in the fracture zone may vary by 50%. The grid size gradients of this magnitude cause an unavoidable scatter of the deformation parameters calculated from the grid images at or near the fracture plane. The occurrence of a gradient could be monitored by using strain measurements on an area rather than a point, but these measurements are more labor intensive. However, it could be a recommendation for future research.

6. CONCLUSIONS

1) The failure of the sheet metal may occur along a direction which is neither the zero extension nor the principal direction of deformation.

2) In a multistage process only the state and strain increments have physical significance -- not the total strain. The stress state in multistage processes can be associated with an equivalent proportional total strain, but such a strain has no physical occurrence.

3) When principal stresses near the fracture zone are transformed to the fracture plane, the resultant normal and shear stresses tend to collapse to a localized region in $\sigma_{xx} - \tau_{xy}$ space.

4) A stress based fracture criterion based on a simple tension-shear stress state rather than principal stress components may exist for sheet metal subjected to multistage deformation processes.

5) Experimental verification of the stress based failure criterion requires precise deformation measurements.

7. ACKNOWLEDGEMENTS

The authors would like to thank the management of Corus for their support in this collaborative project.

8. REFERENCES

1. R. Arrieux, C. Bedrin, M. Boivin, "Determination of an intrinsic forming limit stress diagram for isotropic sheets", *Proc 12th IDDRG Congress*, Sta. Margherita Ligure, 1982, 61-71.
2. L. Zhao, R. Sowerby, M.P. Sklad, "A theoretical and experimental investigation of limit strains in sheet metal forming", *Int. J. Mech. Sci.*, 1996, 38, 1307-1317
3. T.B. Stoughton, "A general forming limit criterion for sheet metal forming" *Int. J. Mech. Sci.*, 2000, 42-1, 1-27.
4. M.P. Sklad, B.A. Yungblud, "Analysis of Multioperation Forming Processes", in *Numerical Methods in Industrial Forming Processes- Numiform 92*, edited by J.L. Chenot, R.D. Woods and O.C. Zienkiewicz, Valbone, France. 1992, 543-549.
5. M.P. Sklad, E.H. Atzema, F.J. Schouten, M. de Bruine and A. Emrich "Experimental Study of forming limits in multistage deformation processes", *Best in Class Stamping - Proceedings of the IDDRG 2008 Int. Conference*, Olofstrom, Sweden, 2008, 721-732.
6. R. Hill, *The Mathematical Theory of Plasticity*, Oxford University Press, 1967, 323-325.
7. Eisso H. Atzema, Ardy Duwel, Louisa Elliott, Peter F. Neve, Henk Vegter, "Appreciation of the Determination of the Forming Limit Curve", *Numisheet 2002*, Jeju, Korea, 2002
8. S.P. Keeler, W.G. Brazier, "Relationship Between Laboratory Material Properties and Press Shop Formability", *Proc Conf. Microalloy 75*, 1977, 517-528.
9. O. Mohr, "Welch Umstände bedingen die Elastizitätsgrenze und den Bruch eines Materials?", *Zeitschrift des Vereins deutscher Ingenieure*, 1900, 44, 1524-1530.